Available online at www.sciencedirect.com
SCIENCE DIRECT®
Journal of Computational Physics 211 (2006) 448–472
JOURNAL OF COMPUTATIONAL PHYSICS
www.elsevier.com/locate/jcp

Multi-symplectic Runge–Kutta methods for nonlinear Dirac equations ☆

Jialin Hong [a,*], Chun Li [a,b]

[a] State Key Laboratory of Scientific and Engineering Computing, Institute of Computational Mathematics and Scientific/Engineering Computing, Academy of Mathematics and Systems Science, Chinese Academy of Sciences, P.O. Box 2719, Beijing 100080, PR China
[b] Graduate School of the Chinese Academy of Sciences, Beijing 100080, PR China

Received 5 August 2004; received in revised form 6 June 2005; accepted 7 June 2005
Available online 22 July 2005

Abstract

In this paper, we consider the multi-symplectic Runge–Kutta (MSRK) methods applied to the nonlinear Dirac equation in relativistic quantum physics, based on a discovery of the multi-symplecticity of the equation. In particular, the conservation of energy, momentum and charge under MSRK discretizations is investigated by means of numerical experiments and numerical comparisons with non-MSRK methods. Numerical experiments presented reveal that MSRK methods applied to the nonlinear Dirac equation preserve exactly conservation laws of charge and momentum, and conserve the energy conservation in the corresponding numerical accuracy to the method utilized. It is verified numerically that MSRK methods are stable and convergent with respect to the conservation laws of energy, momentum and charge, and MSRK methods preserve not only the inner geometric structure of the equation, but also some crucial conservative properties in quantum physics. A remarkable advantage of MSRK methods applied to the nonlinear Dirac equation is the precise preservation of charge conservation law.

Keywords: Multi-symplectic Runge–Kutta methods; Conservation laws; Nonlinear Dirac equations

1. Introduction

As well known, the Dirac equation is the most important mathematical model in relativistic quantum physics. Some authors have considered numerical methods for solving the equation, such as spectral

☆ This work is supported by the Director Innovation Foundation of ICMSEC and AMSS, the Foundation of CAS, the NNSFC (Nos. 19971089 and 10371128) and the Special Funds for Major State Basic Research Projects of China G1999032804.
* Corresponding author.
E-mail addresses: hjl@lsec.cc.ac.cn (J. Hong), lichun@lsec.cc.ac.cn (C. Li).

0021-9991/$ - see front matter © 2005 Elsevier Inc. All rights reserved.
doi:10.1016/j.jcp.2005.06.001

methods (see [5]) and finite difference methods including conservative type methods (see [1–3]). Recently, the multi-symplectic methods have been proposed and investigated for some important Hamiltonian partial differential equations (HPDEs), such as Schrödinger equations [15], KdV equations [15], etc. Some basic results on the methods have been presented. The theoretical framework on generalizing symplectic integrators of Hamiltonian systems to multi-symplectic integrators of HPDEs is established in [4,13,14] and references therein. In [16,17,19], the multi-symplecticity of Gauss–Legendre methods is proven, and the backward error analysis is considered. The classical conservative properties of multi-symplectic methods are investigated in [8,9,11,12]. In particular, it is shown in [18] that a standard second-order finite difference uniform space discretization of the semilinear wave equation with periodic boundary conditions, analytic nonlinearity, and analytic initial data conserves momentum up to an error which is exponentially small in the stepsize. In [9], it is shown that the MSRK methods applied to the nonlinear Dirac equations are stable and convergent with respect to the conservation laws of energy, momentum and charge. Based on the theoretical results presented in [9], in this paper we introduce and numerically investigate some properties of MSRK methods applied to the Dirac equations. In particular, we pay our attention to the preservation of classical conservative properties which is crucial in the numerical study of quantum physics. This paper is organized as follows, in the rest of this section, we introduce $(1+1)$-dimensional nonlinear Dirac equation and the charge conservation law; we propose the multi-symplecticity and energy, and momentum conservation laws of the equation in Section 2; in Section 3, we recall the definition of multi-symplectic discretization for the general HPDEs, and present the condition of multi-symplecticity of Runge–Kutta discretization for HPDEs which has been proven in [6], and state some basic properties of MSRK methods for HPDEs; in Section 4, we restate some results (in [9]) on the discrete charge conservation law, error estimates of energy conservation and momentum conservation for nonlinear Dirac equations under MSRK discretization; numerical experiments and numerical comparisons between a MSRK method and a non-MSRK method are presented in Section 5. The conclusion of this paper is given in Section 6.

We consider $(1+1)$-dimensional nonlinear Dirac equation:

$$\begin{cases} \psi_t = A\psi_x + \mathrm{i}f(|\psi_1|^2 - |\psi_2|^2)B\psi, \\ \psi_1(x,0) = \phi_1(x), \quad \psi_2(x,0) = \phi_2(x), \end{cases} \tag{1.1}$$

where $\psi = (\psi_1,\psi_2)^{\mathrm{T}}$ is a spinorial wave function, which describes a particle with the spin-$\frac{1}{2}$; ψ_1 and ψ_2 are complex functions, which describe the up and down states of the spin-$\frac{1}{2}$ particle, respectively, each of them has two components, denoted by the real and imaginary parts of the complex function, respectively (for more details, see [1–3,5]); $\mathrm{i} = \sqrt{-1}$ is the imaginary unit, $f(s)$ is a real function of a real variable s, A and B are matrices

$$A = \begin{pmatrix} 0 & -1 \\ -1 & 0 \end{pmatrix}, \quad B = \begin{pmatrix} -1 & 0 \\ 0 & 1 \end{pmatrix},$$

the initial function $\phi = (\phi_1,\phi_2)^{\mathrm{T}}$ is sufficiently smooth.

Since a spin-$\frac{1}{2}$ particle has not only the information of energy and momentum, but also the probability information. The concept of probability is derived from the quantum theory. In this context, the charge (the probability information) $\mathscr{Q}$, the linear momentum $\mathscr{P}$ and the energy $\tilde{E}$ are given by:

$$\begin{cases} \mathscr{Q}(\psi)(t) = \int_R (|\psi_1(x,t)|^2 + |\psi_2(x,t)|^2)\,\mathrm{d}x, \\ \mathscr{P}(\psi)(t) = \int_R \Im(\bar{\psi}_1 \frac{\partial}{\partial x}\psi_1 + \bar{\psi}_2 \frac{\partial}{\partial x}\psi_2)\,\mathrm{d}x, \\ \tilde{E}(\psi)(t) = \int_R (\Im(\bar{\psi}_1 \frac{\partial}{\partial x}\psi_2 + \bar{\psi}_2 \frac{\partial}{\partial x}\psi_1) + \tilde{f}(|\psi_1|^2 - |\psi_2|^2))\,\mathrm{d}x, \end{cases} \tag{1.2}$$

respectively, where $\Im(u)$ and $\bar{u}$ denote the imaginary part and the conjugate of the complex u, respectively, $\tilde{f}$ is a primitive function of f, namely

$$\tilde{f}(s) = \int_0^s f(\tau)\,\mathrm{d}\tau.$$

In this paper, we will focus on an important particular case of (1.1):

$$\begin{cases} \frac{\partial \psi_1}{\partial t} + \frac{\partial \psi_2}{\partial x} + \mathrm{i}m\psi_1 + 2\mathrm{i}\lambda(|\psi_2|^2 - |\psi_1|^2)\psi_1 = 0, \\ \frac{\partial \psi_2}{\partial t} + \frac{\partial \psi_1}{\partial x} - \mathrm{i}m\psi_2 + 2\mathrm{i}\lambda(|\psi_1|^2 - |\psi_2|^2)\psi_2 = 0, \end{cases} \tag{1.3}$$

that is,

$$f(s) = m - 2\lambda s$$

in (1.1), where m and λ are real constants. The results obtained can be easily extended to the general case (1.1).

Proposition 1.1. *If the solution ψ of the Dirac equation (1.3) satisfies*

$$\lim_{|x|\to+\infty} |\psi(x,t)| = 0, \quad \textit{uniformly for} \quad t \in R, \tag{1.4}$$

then

$$\mathcal{Q}(\psi)(t) = \mathcal{Q}(\phi), \tag{1.5}$$

where

$$\mathcal{Q}(\phi)(t) = \int_R (|\phi_1|^2 + |\phi_2|^2)\,\mathrm{d}x. \tag{1.6}$$

Proof. Differentiating the first equation of (1.2) with respect to t, we have

$$\frac{\mathrm{d}}{\mathrm{d}t}\mathcal{Q}(\psi) = \int_R \left(\bar{\psi}_1 \frac{\partial}{\partial_t}\psi_1 + \psi_1 \frac{\partial}{\partial t}\bar{\psi}_1 + \bar{\psi}_2 \frac{\partial}{\partial t}\psi_2 + \psi_2 \frac{\partial}{\partial_t}\bar{\psi}_2 \right) \mathrm{d}x. \tag{1.7}$$

From the first equation of (1.3), it follows that

$$\bar{\psi}_1 \frac{\partial}{\partial t}\psi_1 + \psi_1 \frac{\partial}{\partial t}\bar{\psi}_1 = -\bar{\psi}_1 \frac{\partial \psi_2}{\partial x} - \psi_1 \frac{\partial \bar{\psi}_2}{\partial x}. \tag{1.8}$$

Similarly, by using the second equation of Eq. (1.3), we have

$$\bar{\psi}_2 \frac{\partial}{\partial t}\psi_2 + \psi_2 \frac{\partial}{\partial t}\bar{\psi}_2 = -\bar{\psi}_2 \frac{\partial \psi_1}{\partial x} - \psi_2 \frac{\partial \bar{\psi}_1}{\partial x}. \tag{1.9}$$

Substituting (1.8) and (1.9) into (1.7) leads to (1.5). The proof is finished. □

The Dirac equation can be deduced from the time-dependent Schrödinger equation, $|\psi_1|^2$ and $|\psi_2|^2$ represent the probability density of the particle being in the two states, respectively, the charge conservation law represents the probability conservation, it is an important conservative quantity in quantum physics.

2. Multi-symplecticity of the Dirac equation

In this section, we describe the multi-symplectic structure, the energy conservation law and the momentum conservation law of the nonlinear Dirac equation (1.3). We rewrite the complex two-component

spinorial wave function as real four-component form, that is, let $\psi_1 = p_1 + \mathrm{i}q_1$, $\psi_2 = p_2 + \mathrm{i}q_2$. Here, p_k and q_k are real functions ($k = 1, 2$) as required above. Now replacing ψ_k in (1.3) by p_k and q_k, leads to:

$$\begin{cases} \frac{\partial p_1}{\partial t} + \frac{\partial p_2}{\partial x} - mq_1 - 2\lambda(p_2^2 + q_2^2 - p_1^2 - q_1^2)q_1 = 0, \\ \frac{\partial q_1}{\partial t} + \frac{\partial q_2}{\partial x} + mp_1 + 2\lambda(p_2^2 + q_2^2 - p_1^2 - q_1^2)p_1 = 0, \\ \frac{\partial p_2}{\partial t} + \frac{\partial p_1}{\partial x} + mq_2 + 2\lambda(p_2^2 + q_2^2 - p_1^2 - q_1^2)q_2 = 0, \\ \frac{\partial q_2}{\partial t} + \frac{\partial q_1}{\partial x} - mp_2 - 2\lambda(p_2^2 + q_2^2 - p_1^2 - q_1^2)p_2 = 0. \end{cases} \tag{2.1}$$

We find that (1.3) can be written as

$$Mz_t + Kz_x = \nabla_z S(z) \tag{2.2}$$

with the state variable $z = (p_1, q_1, p_2, q_2)^{\mathrm{T}}$, here we use the real vector function z to substitute the complex wave function ψ for latter discussions. M and K are skew-symmetric matrices,

$$M = \begin{pmatrix} 0 & 1 & 0 & 0 \\ -1 & 0 & 0 & 0 \\ 0 & 0 & 0 & 1 \\ 0 & 0 & -1 & 0 \end{pmatrix}, \quad K = \begin{pmatrix} 0 & 0 & 0 & 1 \\ 0 & 0 & -1 & 0 \\ 0 & 1 & 0 & 0 \\ -1 & 0 & 0 & 0 \end{pmatrix},$$

and S: $R^4 \to R$ is a smooth function,

$$S(z) = \frac{1}{2}(\lambda(p_1^2 + q_1^2 - p_2^2 - q_2^2) - m)(p_1^2 + q_1^2 - p_2^2 - q_2^2).$$

In terms of (1.1), we can get the initial condition

$$z_f(x) = z(x, 0) = (\phi_{11}(x), \phi_{12}(x), \phi_{21}(x), \phi_{22}(x))^{\mathrm{T}}, \tag{2.3}$$

where $\phi_1(x) = \phi_{11}(x) + \mathrm{i}\phi_{12}(x)$, $\phi_2(x) = \phi_{21}(x) + \mathrm{i}\phi_{22}(x)$.

According to [4,19] and references therein, the above system (2.2) is called multi-symplectic Hamiltonian system, because it has a multi-symplectic conservation law

$$\frac{\partial \omega}{\partial t} + \frac{\partial \kappa}{\partial x} = 0, \tag{2.4}$$

where ω and κ are pre-symplectic forms,

$$\omega = \frac{1}{2}\,\mathrm{d}z \wedge M\,\mathrm{d}z \quad \text{and} \quad \kappa = \frac{1}{2}\,\mathrm{d}z \wedge K\,\mathrm{d}z. \tag{2.5}$$

The system has an energy conservation law (ECL)

$$\frac{\partial E}{\partial t} + \frac{\partial F}{\partial x} = 0 \tag{2.6}$$

with energy density

$$E = S(z) - \frac{1}{2}z^{\mathrm{T}}Kz_x$$

and energy flux

$$F = \frac{1}{2}z^{\mathrm{T}}Kz_t.$$

From the energy formula in (1.2) and comparing with the energy density given here, it follows that

$$\Im\left(\bar{\psi}_1\frac{\partial}{\partial x}\psi_2+\bar{\psi}_2\frac{\partial}{\partial x}\psi_1\right)+\tilde{f}(|\psi_1|^2-|\psi_2|^2)=-2E,$$

that is,

$$\tilde{E}(\psi)(t)=-2\int_R E(z(x,t))\,\mathrm{d}x. \tag{2.7}$$

The system has also a momentum conservation law (MCL)

$$\frac{\partial I}{\partial t}+\frac{\partial G}{\partial x}=0 \tag{2.8}$$

with momentum density

$$I=\frac{1}{2}z^{\mathrm{T}}Mz_x$$

and momentum flux

$$G=S(z)-\frac{1}{2}z^{\mathrm{T}}Mz_t.$$

Similarly, corresponding to the linear formula given in (1.2), we obtain

$$\Im\left(\bar{\psi}_1\frac{\partial}{\partial x}\psi_1+\bar{\psi}_2\frac{\partial}{\partial x}\psi_2\right)=2I,$$

namely

$$\mathscr{P}(\psi)(t)=2\int_R I(z(x,t))\,\mathrm{d}x. \tag{2.9}$$

Three conservation laws (2.4), (2.6) and (2.8) are the local properties which hold for any multi-symplectic system (see [4]), in general, they could not provide more information on the global properties of the system. Under appropriate assumptions, it is possible to gain the global conservation laws corresponding to the local conservative properties.

Proposition 2.1. *Under the assumptions of Proposition* 1.1, *and if*

$$\lim_{|x|\to+\infty}|\partial_x\psi(x,t)|=0\quad \textit{uniformly for}\quad t\in R, \tag{2.10}$$

then the system (1.3) *has two conservation laws*:

$$\mathscr{P}(\psi)(t)=\mathscr{P}(\phi), \tag{2.11}$$

$$\tilde{E}(\psi)(t)=\tilde{E}(\phi) \tag{2.12}$$

on the linear momentum and the energy as mentioned in Section 1, *respectively*, *where*:

$$\mathscr{P}(\phi)(t)=\int_R\Im\left(\bar{\phi}_1\frac{\partial}{\partial x}\phi_1+\bar{\phi}_2\frac{\partial}{\partial x}\phi_2\right)\mathrm{d}x, \tag{2.13}$$

$$\tilde{E}(\phi)(t)=\int_R\left(\Im\left(\bar{\phi}_1\frac{\partial}{\partial x}\phi_2+\bar{\phi}_2\frac{\partial}{\partial x}\phi_1\right)+\tilde{f}(|\phi_1|^2-|\phi_2|^2)\right)\mathrm{d}x. \tag{2.14}$$

Proof. We integrate (2.6) over R, then

$$\int_R \left(\frac{\partial E}{\partial t} + \frac{\partial F}{\partial x}\right) \mathrm{d}x = 0. \tag{2.15}$$

(2.2) implies that

$$z_t = M^{-1}(\nabla_z S(z) - K z_x) = -M\nabla_z S(z) + M K z_x, \tag{2.16}$$

since $\nabla_z S(z)$ is a vector function, each of whose entries is a multivariable polynomial with the degree 3, under the assumptions of this proposition, it is concluded that

$$\lim_{|x|\to+\infty} \nabla_z S(z) = 0 \quad \text{and} \quad \lim_{|x|\to+\infty} z_x = 0. \tag{2.17}$$

Therefore, (2.16) and (2.17) imply

$$\lim_{|x|\to+\infty} z_t = 0. \tag{2.18}$$

The left term of (2.15) can be written as

$$\int_R \left(\frac{\partial E}{\partial t} + \frac{\partial F}{\partial x}\right) \mathrm{d}x = \frac{\mathrm{d}}{\mathrm{d}t}\int_R E\,\mathrm{d}x + \left(\frac{1}{2} z^{\mathrm{T}} K z_t\right)\Big|_{-\infty}^{+\infty} = \frac{\mathrm{d}}{\mathrm{d}t}\int_R E\,\mathrm{d}x. \tag{2.19}$$

Combining (2.7), we find that $\frac{\mathrm{d}}{\mathrm{d}t}\tilde{E}(\psi)(t) = 0$, which shows that (2.12) holds, namely, we have obtained the energy conservation law. Similarly, combining (2.9) and the local momentum conservation law (2.8), the momentum conservation law can be obtained. This completes the proof. □

Because numerical methods should preserve characteristic properties and inner structures (symmetries) of original system as much as possible, it would be very important to find more numerical methods which preserve multi-symplectic conservation law (2.4) for Hamiltonian systems (2.2).

3. Multi-symplectic Runge–Kutta methods

In this section, we introduce multi-symplecticity of numerical methods and recall the condition of multi-symplecticity of Runge–Kutta discretization for general HPDEs and some known results. In order to process the numerical discretization, we introduce a uniform grid [10] $(x_j,t_k) \in R^2$ with mesh-length Δt in the t-direction and mesh-length Δx in the x-direction, and denote the value of the function $\psi(x,t)$ at the mesh point (x_j,t_k) by ψ_j^k. Eq. (2.2) and the multi-symplectic conservation law (2.4) can be, respectively, schemed numerically as:

$$M\partial_t^{j,k} z_j^k + K\partial_x^{j,k} z_j^k = (\nabla_z S(z))_j^k, \tag{3.1}$$

$$\partial_t^{j,k}\omega_j^k + \partial_x^{j,k}\kappa_j^k = 0, \tag{3.2}$$

where $(\nabla_z S(z))_j^k = (\nabla_z S(z_j^k))$,

$$\omega = \frac{1}{2}(\mathrm{d}z)_j^k \wedge M(\mathrm{d}z)_j^k \quad \text{and} \quad \kappa = \frac{1}{2}(\mathrm{d}z)_j^k \wedge K(\mathrm{d}z)_j^k,$$

where $\partial_t^{j,k}$ and $\partial_x^{j,k}$ are discretizations of the partial derivatives ∂_t and ∂_x, respectively.

Definition 3.1. The numerical scheme (3.1) of (2.2) is said to be multi-symplectic if (3.2) is a discrete conservation law of (3.1).

In [19], Reich shows that the Gauss–Legendre discretization applied to the scalar wave equation (and Schrödinger equation) both in time and space direction, leads to a multi-symplectic integrator (also see [11]). Hong et al. [6] presents the condition of multi-symplecticity of Runge–Kutta methods and partitioned Runge–Kutta methods for the general Hamiltonian partial differential equations in the form (2.2).

Now we recall the characterization of multi-symplectic Runge–Kutta methods for the general Hamiltonian partial differential equations in the form (2.2). To simplify notations, let the starting point $(x_0,t_0) = (0,0)$. Applying r-stage and s-stage RK methods to the multi-symplectic system (2.2) in the t-direction and x-direction, respectively, we have the following:

$$\begin{cases} Z_m^k = z_m^0 + \Delta t \sum_{j=1}^{r} a_{kj} \partial_t Z_m^j, \\ z_m^1 = z_m^0 + \Delta t \sum_{k=1}^{r} b_k \partial_t Z_m^k, \\ Z_m^k = z_0^k + \Delta x \sum_{n=1}^{s} \tilde{a}_{mn} \partial_x Z_n^k, \\ z_1^k = z_0^k + \Delta x \sum_{m=1}^{s} \tilde{b}_m \partial_x Z_m^k, \\ M \partial_t Z_m^k + K \partial_x Z_m^k = \nabla_z S(Z_m^k), \end{cases} \tag{3.3}$$

here, we made use of the following notations: $Z_m^k \approx z(c_m\Delta t, d_k\Delta x)$, $z_m^0 \approx z(c_m\Delta x, 0)$, $\partial_t Z_m^k \approx \partial_t z(c_m\Delta x, d_k\Delta t)$, $\partial_x Z_m^k \approx \partial_x z(c_m\Delta x, d_k\Delta t)$, $z_m^1 \approx z(c_m\Delta x, \Delta t)$, $z_0^k \approx z(0, d_k\Delta t)$, $z_1^k \approx z(\Delta x, d_k\Delta t)$, and

$$c_m = \sum_{n=1}^{s} \tilde{a}_{mn}, \quad d_k = \sum_{j=1}^{r} a_{kj}.$$

The variational equation corresponding to (3.3) is:

$$\begin{cases} \mathrm{d}Z_m^k = \mathrm{d}z_m^0 + \Delta t \sum_{j=1}^{r} a_{kj}\, \mathrm{d}(\partial_t Z)_m^j, \\ \mathrm{d}z_m^1 = \mathrm{d}z_m^0 + \Delta t \sum_{k=1}^{r} b_k\, \mathrm{d}(\partial_t Z)_m^k, \\ \mathrm{d}Z_m^k = \mathrm{d}z_0^k + \Delta x \sum_{n=1}^{s} \tilde{a}_{mn}\, \mathrm{d}(\partial_x Z)_n^k, \\ \mathrm{d}z_1^k = \mathrm{d}z_0^k + \Delta x \sum_{m=1}^{s} \tilde{b}_m\, \mathrm{d}(\partial_x Z)_m^k, \\ M\, \mathrm{d}(\partial_t Z)_m^k + K\, \mathrm{d}(\partial_x Z)_m^k = D_{zz} S(Z_m^k)\, \mathrm{d}Z_m^k, \end{cases} \tag{3.4}$$

where we use the abbreviations, $\mathrm{d}Z_m^k$ denotes $(\mathrm{d}Z)_m^k$, $\mathrm{d}(\partial_t Z)_m^k$ denotes $(\mathrm{d}(\partial_t Z))_m^k$ and so on.

Based on the discrete formula (3.2) of the multi-symplectic conservation law, we consider the multi-symplecticity of Runge–Kutta methods. Making use of the variational equation (3.4), after a tedious calculation, we have

$$\Delta x\sum_{m=1}^{s}\tilde{b}_m(\mathrm{d}z_m^1\wedge M\mathrm{d}z_m^1-\mathrm{d}z_m^0\wedge M\mathrm{d}z_m^0)+\Delta t\sum_{k=1}^{r}b_k(\mathrm{d}z_1^k\wedge K\mathrm{d}z_1^k-\mathrm{d}z_0^k\wedge K\mathrm{d}z_0^k)$$
$$=\Delta x\Delta t^2\sum_{m=1}^{s}\tilde{b}_m\sum_{k=1}^{r}\sum_{j=1}^{r}(b_kb_j-b_ka_{kj}-b_ja_{jk})\,\mathrm{d}(\partial_tZ)_m^k\wedge M\,\mathrm{d}(\partial_tZ)_m^j$$
$$+\Delta x^2\Delta t\sum_{k=1}^{r}b_k\sum_{k=1}^{r}\sum_{j=1}^{r}(\tilde{b}_m\tilde{b}_n-\tilde{b}_m\tilde{a}_{mn}-\tilde{b}_n\tilde{a}_{nm})\,\mathrm{d}(\partial_xZ)_m^k\wedge K\,\mathrm{d}(\partial_xZ)_n^k,$$

hence we derive the following theorem (for more details of the proof, see [6,19]).

Theorem 3.2. [6] *If the method (3.3) satisfies the following coefficient conditions*:

$$\begin{cases}b_kb_j-b_ka_{kj}-b_ja_{jk}=0,\\ \tilde{b}_m\tilde{b}_n-\tilde{b}_m\tilde{a}_{mn}-\tilde{b}_n\tilde{a}_{nm}=0\end{cases}\tag{3.5}$$

for all $k,j=1,2,\ldots,r$ *and* $m,n=1,\ldots,s$, *then (3.3) is multi-symplectic with the discrete multi-symplectic conservation law*

$$\Delta x\sum_{m=1}^{s}\tilde{b}_m(\omega_m^1-\omega_m^0)+\Delta t\sum_{k=1}^{r}b_k(\kappa_1^k-\kappa_0^k)=0,\tag{3.6}$$

where $\omega_m^1=\frac{1}{2}\mathrm{d}z_m^1\wedge M\mathrm{d}z_m^1$, $\kappa_1^k=\frac{1}{2}\mathrm{d}z_1^k\wedge K\mathrm{d}z_1^k$, $\omega_m^0=\frac{1}{2}\mathrm{d}z_m^0\wedge M\mathrm{d}z_m^0$, $\kappa_0^k=\frac{1}{2}\mathrm{d}z_0^k\wedge K\mathrm{d}z_0^k$.

Theorem 3.2 tells us that the symplectic Runge–Kutta discretization applied to the Hamiltonian partial differential equation (2.2) in both time and space direction, leads to a multi-symplectic integrator. For any HPDE, there are three local conservation laws, (2.4), (2.6) and (2.8). Eq. (3.6) in Theorem 3.2 is the discrete analogue of (2.4).

Now there is a natural question: *Do MSRK methods preserve* (2.6) and (2.8) *in the sense of the corresponding discretization?* Reich [19] shows that Gauss–Legendre schemes preserve exactly both of the energy conservation law and the momentum conservation law for the linear wave equation, and numerical experiments therein show that Gauss–Legendre methods, for nonlinear wave equations, preserve the conservation laws of energy and momentum in a good approximation. Bridges and Reich [4] show that if $S(z)$ is quadratic in z, then the multi-symplectic box scheme conserves exactly the conservation laws of local energy and local momentum. Islas et al. [11] show that the multi-symplectic box schemes can give good approximations of the discrete energy and discrete momentum, respectively, for the nonlinear Schrödinger equation. Hong et al. [6] give the following result.

Theorem 3.3. [6] *For any general multi-symplectic system, if* $S(z)=\frac{1}{2}z^{\mathrm{T}}Hz$, *where* H *is any symmetric matrix, and the coefficient matrices of RK methods* $A=(a_{kj})_{r\times r}$ *and* $\tilde{A}=(\tilde{a}_{mn})_{s\times s}$ *in (3.3) satisfying (3.5) are invertible, then the method (3.3) has a discrete energy conservation law*

$$\Delta x\sum_{m=1}^{s}\tilde{b}_m\big(E(z_m^1)-E(z_m^0)\big)+\Delta t\sum_{k=1}^{r}b_k\big(F(z_1^k)-F(z_0^k)\big)=0$$

and a discrete momentum conservation law

$$\Delta x\sum_{m=1}^{s}\tilde{b}_m\big(I(z_m^1)-I(z_m^0)\big)+\Delta t\sum_{k=1}^{r}b_k\big(G(z_1^k)-G(z_0^k)\big)=0.$$

4. The statement of discrete conservative properties

In [9,12,16,17], discrete conservative properties of some multi-symplectic integrators have been investigated. When a MSRK method is applied to the nonlinear Dirac equations, an important problem is, *does it preserve the physical conservative properties, such as conservation laws of charge, energy and momentum in the global sense ((2.12), (2.11) and (1.5), respectively), of the equation?* In this section, we recall some results presented in [9] which solve the above problem. In what follows, we assume that the Runge–Kutta methods considered are solvable, and satisfy the condition (3.5) of multi-symplecticity.

Now we replace the whole real spatial region R by a finite interval $[-L/2,L/2]$. An initial condition is taken as

$$z(x,0) = z_f(x),$$

where $z_f(x)$ is the same as (2.3). The investigation of the global conservation properties requires that $z_f(x)$ satisfies periodic boundary condition on the interval $[-L/2,L/2]$, namely $z_f(-L/2) = z_f(L/2)$. The consistent periodic boundary condition is given by

$$z(-L/2,t) = z(L/2,t) \quad \text{or} \quad z(-L/2,t) = z(L/2,t) = z_b(t),$$

where $z_b(t)$ is a known real-valued and sufficiently smooth vector function. Set the spatial points $x_l = -L/2 + lL/N$, $l = 0,1,\ldots,N$. Let the starting time point $t_0 = 0$, and let $\tau = \Delta t$ and $h = \Delta x = L/N$ be the time step and spatial step, respectively, we rewrite the Runge–Kutta method (3.3) over all spatial points as follows:

$$\begin{cases} Z^k_{l,m} = z^0_{l,m} + \tau \sum_{j=1}^{r} a_{kj} \partial_t Z^j_{l,m}, \\ z^1_{l,m} = z^0_{l,m} + \tau \sum_{k=1}^{r} b_k \partial_t Z^k_{l,m}, \\ Z^k_{l,m} = z^k_{l,0} + h \sum_{n=1}^{s} \tilde{a}_{mn} \partial_x Z^k_{l,n}, \\ z^k_{l+1,0} = z^k_{l,0} + h \sum_{m=1}^{s} \tilde{b}_m \partial_x Z^k_{l,m}, \\ M \partial_t Z^k_{l,m} + K \partial_x Z^k_{l,m} = \nabla_z S(Z^k_{l,m}), \end{cases} \tag{4.1}$$

where $k = 1,\ldots,r$, $m = 1,\ldots,s$, $l = 0,1,\ldots,N-1$, $Z^k_{l,m} \approx z((l+c_m)h, d_k\tau)$, $z^0_{l,m} \approx z((l+c_m)h, 0)$, $z^k_{l,0} \approx z(lh, d_k\tau)$ and so on.

4.1. The discrete charge conservation law of MSRK methods

It follows from Proposition 1.1 that the charge conservation law of the Hamiltonian PDE (2.2) is the following:

$$\mathcal{Q}(z)(t) = \mathcal{Q}(z_f), \tag{4.2}$$

where $\mathcal{Q}(z)(t) = \int_{-L/2}^{L/2} z(x,t)^{\mathrm{T}} z(x,t)\,\mathrm{d}x$ and $\mathcal{Q}(z_f) = \int_{-L/2}^{L/2} z_f(x)^{\mathrm{T}} z_f(x)\,\mathrm{d}x$.

The conservation of quadratic invariants under the numerical discretization is very important. As well known, in the case of Hamiltonian ODEs symplectic integrators, in general, may not preserve quadratic invariants [20]. The invariance of (4.2) under MSRK discretization is stated in the following result.

Theorem 4.1. [9] *The RK method (3.3) satisfying (3.5) has the following discrete charge conservation law*

$$h\sum_{l=0}^{N-1}\sum_{m=1}^{s}\tilde{b}_m\left(Q_e(z_{l,m}^1)-Q_e(z_{l,m}^0)\right)=0, \tag{4.3}$$

where $Q_e(z)=z^{\mathrm{T}}z$.

This result reveals the stability of MSRK methods applied to the nonlinear Dirac equation in the sense of the charge conservation law (4.2), and ensures that, in the numerical implementation, the normalization of quantum physics is preserved exactly by the MSRK methods.

4.2. The errors of discrete energy and discrete momentum of MSRK methods

Neglecting the integral coefficients -2 and 2 in (2.7) and (2.8), respectively, the corresponding total energy to (2.7) is denoted by

$$\mathscr{E}_L(t)=\int_{-L/2}^{L/2}E(z(x,t))\,\mathrm{d}x \tag{4.4}$$

and the corresponding total momentum to (2.9) by

$$\mathscr{I}_L(t)=\int_{-L/2}^{L/2}I(z(x,t))\,\mathrm{d}x. \tag{4.5}$$

Now we integrate the energy conservation law (2.6) over the local domain, namely

$$\int_0^h[E(z(x,\tau))-E(z(x,0))]\,\mathrm{d}x+\int_0^\tau[F(z(h,t))-F(z(0,t))]\,\mathrm{d}t=0. \tag{4.6}$$

Corresponding to the RK method (3.3), we use a discrete form

$$E_{le}\triangleq h\sum_{m=1}^{s}\tilde{b}_m(E(z_m^1)-E(z_m^0))+\tau\sum_{k=1}^{r}b_k(F(z_1^k)-F(z_0^k)) \tag{4.7}$$

to approximate the left side of (4.6). The following result reveals the preservation of (4.6) when the MSRK methods are applied to the nonlinear Dirac equations.

Theorem 4.2. [9] *If the matrices of RK methods in (3.3) satisfying (3.5) are invertible and the solution* z, $\partial_t z$ *and* $\partial_x z$ *are bounded, then for the method (3.3), the error of the local discrete energy conservation law satisfies*

$$|E_{le}|\leqslant C\tau^3 h \tag{4.8}$$

for sufficiently small τ *and* h, *where the constant* C *is independent of* τ *and* h.

According to (2.12) in Proposition 2.1 and (2.7), we have the total energy conservation law

$$\frac{\mathrm{d}}{\mathrm{d}t}\mathscr{E}_L(t)=0.$$

Corresponding to the RK discretization (4.1), we define the discrete total energy at time t_i as

$$\left(\mathscr{E}_L^d\right)^i=h\sum_{l=0}^{N-1}\sum_{m=1}^{s}\tilde{b}_m E(z_{l,m}^i),$$

where $z_{l,m}^i\approx z(lh+c_m h,i\tau)$ and i is a non-negative integer.

Theorem 4.3. [9] *Under the assumptions of Theorem* 4.2, *the local error of the discrete total energy conservation law satisfies*

$$|E_{te}| \triangleq |(\mathscr{E}_L^d)^1 - (\mathscr{E}_L^d)^0| \leqslant C\tau^3 \tag{4.9}$$

for sufficiently small τ *and* h, *where the constant* C *is independent of* τ *and* h.

Theorem 4.4. [9] *Under the assumptions of Theorem* 4.2, *for* $T > 0$, *there exists a* $\tau_0 > 0$ *and an* $h_0 > 0$, *such that for* $\tau < \tau_0$ *and* $h < h_0$, *the global error of the discrete total energy law satisfies*

$$|(\mathscr{E}_L^d)^n - (\mathscr{E}_L^d)^0| \leqslant C\tau^2 \quad \textit{uniformly for} \quad n\tau \leqslant T, \tag{4.10}$$

where the constant C *is independent of* τ, h *and* T.

It is shown in [18] that on uniform grid of the spatial discretization, the interpolate momentum satisfies an exponential estimate. The result restated here is on the error estimate of total momentum for MSRK methods of the Dirac equation. As discussed in the above energy analysis, we start with the local momentum conservation law first. It follows from (2.8) that

$$\int_0^h [I(z(x,\tau)) - I(z(x,0))]\,\mathrm{d}x + \int_0^\tau [G(z(h,t)) - G(z(0,t))]\,\mathrm{d}t = 0. \tag{4.9}$$

We define

$$M_{le} = h\sum_{m=1}^{s} \tilde{b}_m (I(z_m^1) - I(z_m^0)) + \tau \sum_{k=1}^{r} b_k (G(z_1^k) - G(z_0^k)) \tag{4.11}$$

as the discrete form of the left side of (4.9). Similar to Theorem 4.2, we have

Theorem 4.5. [9] *Under the assumptions of Theorem* 4.2, *the following estimation*

$$|M_{le}| \leqslant C\tau h^3 \tag{4.12}$$

holds for sufficiently small τ *and* h, *where the positive constant* C *is independent of* z, $\partial_t z$, $\partial_x z$, *and* S.

Similarly to the above discussion on total energy conservation law, combining (2.7) and (2.11) in Proposition 2.1, we have the total momentum conservation law

$$\frac{\mathrm{d}}{\mathrm{d}t}\mathscr{I}_L(t) = 0.$$

We define the discrete total energy at time t_i as

$$(\mathscr{I}_L^d)^i = h\sum_{l=0}^{N-1}\sum_{m=1}^{s} \tilde{b}_m I(z_{l,m}^i).$$

As mentioned in the above, Oliver et al. [18] gives an exponential estimate for the total momentum of the semilinear wave equations. From Theorem 4.5, it follows that the local and global errors of the discrete total momentum for nonlinear Dirac equations is of order $\mathcal{O}(\tau h^2)$ and $\mathcal{O}(h^2)$, respectively, under the Runge–Kutta discretization.

4.3. The error estimates of the discrete conservation laws for a non-multi-symplectic method

In this section, we give some theoretical results on the numerical characters of a second-order non-multi-symplectic method TT2 (see Section 5 for more details), and we only focus on the error estimates of discrete

conservation laws. The TT2 has no discrete charge conservation law. Analogous to the discussion in Theorem 4.1, we deduce the following error estimates.

Theorem 4.6. [9] *Under the same boundedness assumptions as in Theorem* 4.2, *for the method TT*2, *we have the following local error estimate on the discrete charge conservation law*

$$\left| h \sum_{l=0}^{N-1} \left(Q_e(z_l^1) - Q_e(z_l^0) \right) \right| \leqslant C\tau(\tau^2 + h^2) \tag{4.13}$$

for sufficiently small τ *and* h, *where* $Q_e(z_l^i) = \left(\frac{z_l^i + z_{l+1}^i}{2}\right)^{\mathrm{T}} \left(\frac{z_l^i + z_{l+1}^i}{2}\right)$ *for* $i = 0, 1$, *and the constant* C *is independent of* τ *and* h.

Theorem 4.7. [9] *Under the assumptions of Theorem* 4.6, *for* $T > 0$, *there exists a* $\tau_0 > 0$ *and an* $h_0 > 0$, *such that for* $\tau < \tau_0$ *and* $h < h_0$, *the global error of the discrete charge conservation law for the TT*2 *method satisfies*

$$\left| h \sum_{l=0}^{N-1} \left(Q_e(z_l^n) - Q_e(z_l^0) \right) \right| \leqslant C(\tau^2 + h^2) \quad \textit{uniformly for} \quad n\tau \leqslant T, \tag{4.14}$$

where the constant C *is independent of* τ, h *and* T.

Theorem 4.8. [9] *Under the assumptions of Theorem* 4.6, *for the method TT*2, *the error of the local discrete energy conservation law satisfies*

$$|E_{le}| \leqslant C\tau h(\tau^2 + h^2) \tag{4.15}$$

for sufficiently small τ *and* h, *where the constant* C *is independent of* τ *and* h.

Theorem 4.9. [9] *Under the assumptions of Theorem* 4.6, *for the method TT*2, *the error of total discrete energy conservation law satisfies*

$$|E_{te}| \leqslant C\tau(\tau^2 + h^2) \tag{4.16}$$

for sufficiently small τ *and* h, *where the constant* C *is independent of* τ *and* h.

Theorem 4.10. [9] *Under the assumptions of Theorem* 4.6, *for* $T > 0$, *there exists a* $\tau_0 > 0$ *and an* $h_0 > 0$, *such that for* $\tau < \tau_0$ *and* $h < h_0$, *the global error of the discrete total energy conservation law for the TT*2 *method satisfies*

$$\left| \left(\mathscr{E}_L^d\right)^n - \left(\mathscr{E}_L^d\right)^0 \right| \leqslant C(\tau^2 + h^2) \quad \textit{uniformly for} \quad n\tau \leqslant T, \tag{4.17}$$

where the constant C *is independent of* τ, h *and* T.

Theorem 4.11. [9] *Under the assumptions of Theorem* 4.6, *for the method TT*2, *the error of local discrete momentum conservation law satisfies*

$$|M_{le}| \leqslant C\tau h(\tau^2 + h^2) \tag{4.18}$$

for sufficiently small τ *and* h, *where the constant* C *is independent of* τ *and* h.

5. Numerical investigation

Based on the theoretical results in the previous section, numerical experiments presented in this section reveal numerical characters of MSRK methods applied to the nonlinear Dirac equations. Without loss of

generality, we take the constants $m = 1$ and $\lambda = \frac{1}{2}$ in (1.3). In this case, the nonlinear Dirac equation (1.3) has the following theoretical solitary wave solution

$$\psi_s(x,t) = (M(x), \mathrm{i}N(x))^{\mathrm{T}} \mathrm{e}^{-\mathrm{i}\Lambda t}, \tag{5.1}$$

where:

$$\begin{cases} M(x) = (2(1-\Lambda^2))^{1/2}(1+\Lambda)^{1/2}\frac{\cosh((1-\Lambda^2)^{1/2}x)}{1+\Lambda\cosh(2(1-\Lambda^2)^{1/2}x)}, \\ N(x) = (2(1-\Lambda^2))^{1/2}(1-\Lambda)^{1/2}\frac{\sinh((1-\Lambda^2)^{1/2}x)}{1+\Lambda\cosh(2(1-\Lambda^2)^{1/2}x)} \end{cases}$$

with the frequency $\Lambda = 0.75$.

We discretize the nonlinear Dirac equation (1.3) by the MSRK method with $r = 1$ and $s = 1$, this is an implicit second-order MSRK method (in short, denoted by MM2), which is equivalent to the central box scheme in [4,7,8,11,12]

$$M\frac{(z_{l+1/2}^{i+1} - z_{l+1/2}^{i})}{\tau} + K\frac{(z_{l+1}^{i+1/2} - z_{l}^{i+1/2})}{h} = \nabla_z S(z_{l+1/2}^{i+1/2}), \tag{5.2}$$

where i and l are indices of the time step and the space step, respectively, and:

$$z_{l+1/2}^{i} = (z_{l+1}^{i} + z_{l}^{i})/2, \quad z_{l+1/2}^{i+1} = (z_{l+1}^{i+1} + z_{l}^{i+1})/2, \quad z_{l}^{i+1/2} = (z_{l}^{i+1} + z_{l}^{i})/2,$$
$$z_{l+1}^{i+1/2} = (z_{l+1}^{i+1} + z_{l+1}^{i})/2, \quad z_{l+1/2}^{i+1/2} = (z_{l+1}^{i+1} + z_{l+1}^{i} + z_{l}^{i+1} + z_{l}^{i})/4.$$

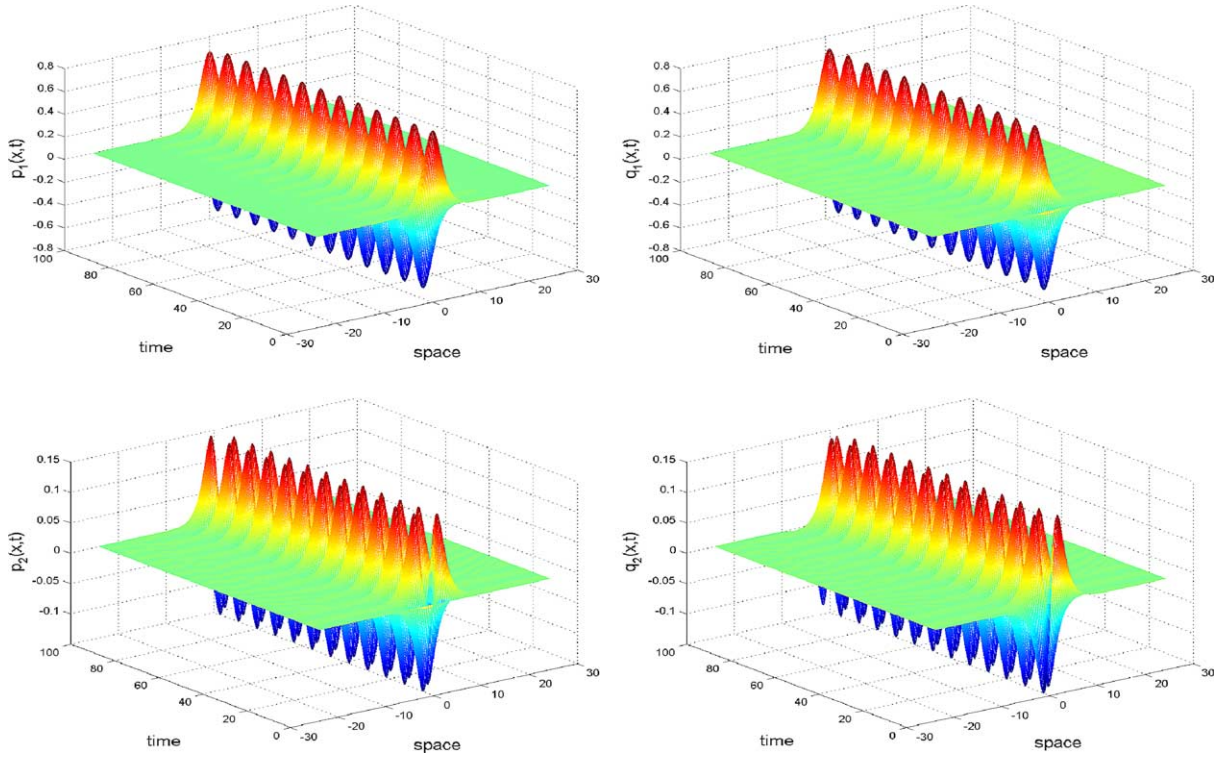

Fig. 1. The four numerical solitary wave functions obtained by using MM2, the left-top one is the first component $p_1(x,t)$, the right-top is the second component $q_1(x,t)$ and the bottom list the third and fourth component $p_2(x,t)$ and $q_2(x,t)$, respectively.

Since $\psi_s(x,t)$ is exponentially small away from $x = 0$, in numerical implementation we take periodic boundary conditions $\psi(-L,t) = \psi(L,t)$ with $L = 24$, and make use of the exact initial conditions:

$$\begin{cases} \phi_1(x) = M(x), \\ \phi_2(x) = \mathrm{i}N(x). \end{cases} \tag{5.3}$$

First, we take the spatial step $h = 0.3$, the time step $\tau = 0.05$, and the time interval is [0,100]. Next, We change the steps or the time interval to check our theoretical results. The fixed point iteration method is utilized to solve the nonlinear algebraic systems generated by the numerical scheme, each iteration will terminate when the maximum absolute error of the adjacent two iterative values is less than 10^{-15}.

For the purpose of numerical comparisons, we apply an implicit second-order non-multi-symplectic method, the trapezoidal scheme in time and space, respectively (in short, denoted by TT2), to the nonlinear Dirac equations. The TT2 is obtained by means of substituting

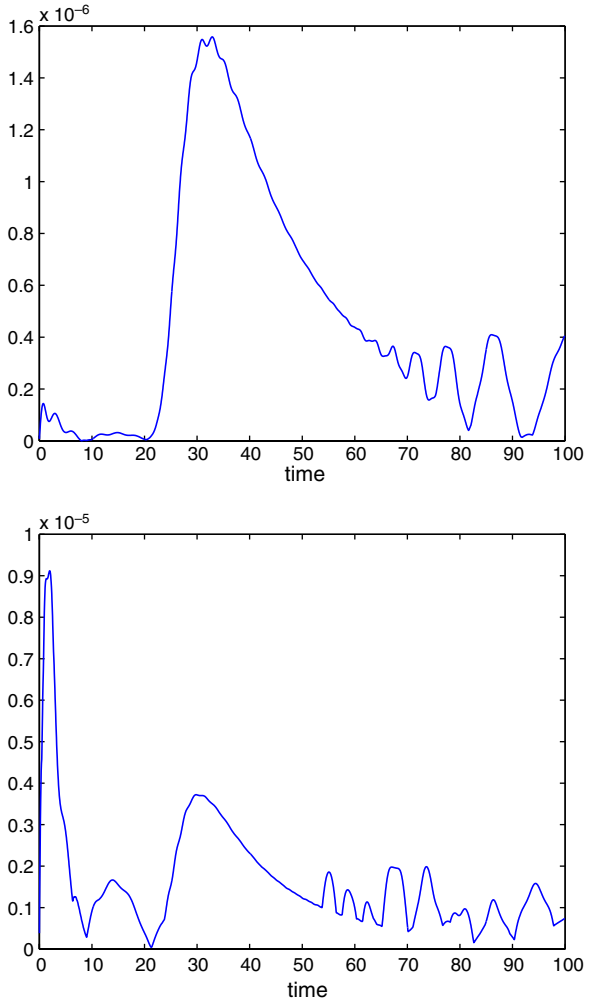

Fig. 2. The maximum errors of the discrete local energy: MM2 (top); TT2 (bottom).

$$\frac{\nabla_z S(z_{l+1}^{i+1}) + \nabla_z S(z_l^{i+1}) + \nabla_z S(z_{l+1}^{i}) + \nabla_z S(z_l^{i})}{4}$$

for the right side of (5.2). All numerical comparisons between MM2 and TT2 are processed in the same numerical conditions.

Fig. 1 shows the numerical result of the spinorial wave function obtained by using MM2. The spatial interval given in the figure is $[-30,30]$ that makes the lower half parts of waves observable. (5.1) tells us that the spinorial wave function is periodic in time, and its period is $2\pi/\Lambda$. Consequently, the time interval $[0,100]$ adopted in the numerical computation contains almost 12 periods, the plots in Fig. 1 show the periodic behavior almost perfectly, the asymptotic behavior of the waves as $x \to \pm\infty$ comports with (5.1). The results of numerical simulation with TT2 are as good as ones with MM2. Especially, MM2 and TT2 have no differences in the cost and the accuracy of numerical computation of solitary waves. We do not plot four figures of numerical results obtained by using the TT2 scheme any more accordingly.

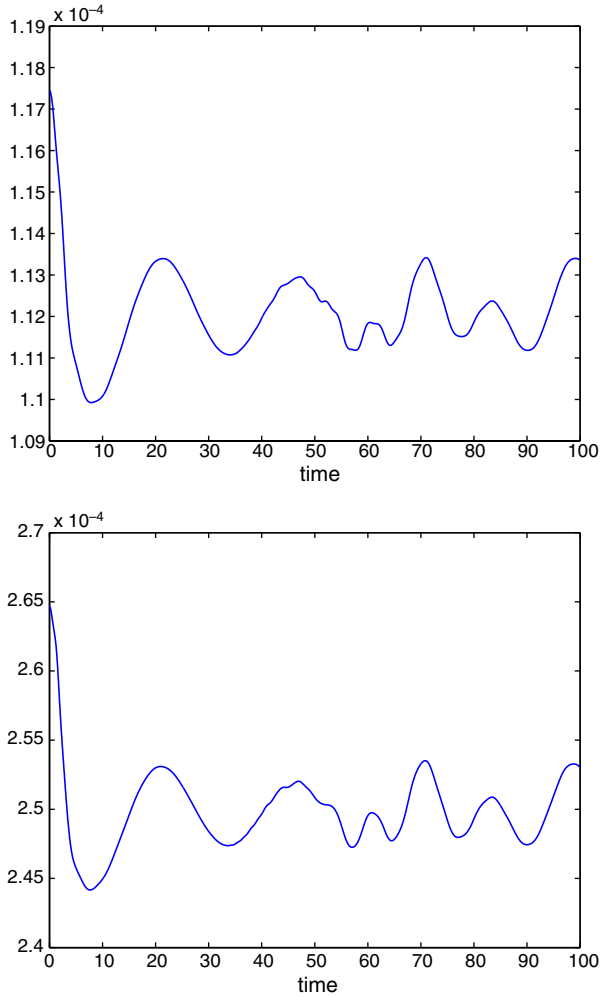

Fig. 3. The maximum errors of the discrete local momentum: MM2 (top); TT2 (bottom).

Because the MSRK methods applied to the nonlinear Dirac equation cannot preserve the energy conservation law exactly, it is important to investigate the error of the energy conservation law. Now we make use of

$$(E_{le}^{*})_{l}^{i} = \sum_{m=1}^{s} \tilde{b}_m \frac{(E(z_{l,m}^{i+1}) - E(z_{l,m}^{i}))}{\tau} + \sum_{k=1}^{r} b_k \frac{(F(z_{l+1}^{i,k}) - F(z_{l}^{i,k}))}{h}$$

to denote the error of the ECL, which is the general form of (4.7) in the rectangle

$$((x_l, t_i), (x_{l+1}, t_i), (x_{l+1}, t_{i+1}), (x_l, t_{i+1})).$$

$(E_{le}^{*})_{l}^{i}$ does not mean the local error at the mesh point (x_l,t_i), since E_{le}^{*} is derived from the local integration E_{le}, and the local integration domain is the rectangle. For the MM2 scheme, $(E_{le}^{*})_{l}^{i}$ is the local error in $(x_{l+1/2}, t_{i+1/2})$, the explicit formula (see [4,11,12]) is

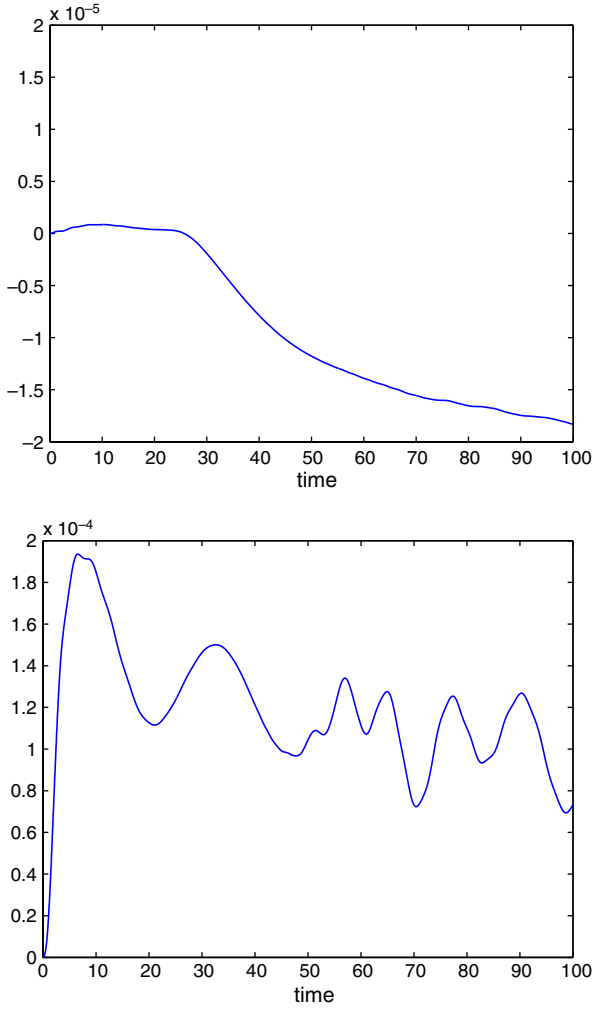

Fig. 4. The global errors of the discrete total energy: MM2 (top); TT2 (bottom).

$$(E^*_{le})^{i+1/2}_{l+1/2} = \frac{1}{\tau}\left[\left(S(z^{i+1}_{l+1/2}) - \frac{1}{2}(z^{i+1}_{l+1/2})^{\mathrm{T}} K \frac{z^{i+1}_{l+1} - z^{i+1}_{l}}{h}\right) - \left(S(z^{i}_{l+1/2}) - \frac{1}{2}(z^{i}_{l+1/2})^{\mathrm{T}} K \frac{z^{i}_{l+1} - z^{i}_{l}}{h}\right)\right] + \frac{1}{h}\left[(z^{i+1/2}_{l+1})^{\mathrm{T}} K \frac{z^{i+1}_{l+1} - z^{i}_{l+1}}{\tau} - (z^{i+1/2}_{l})^{\mathrm{T}} K \frac{z^{i+1}_{l} - z^{i}_{l}}{\tau}\right],$$

where notations are the same as ones in (5.2). Similarly, the error $(M^*_{le})^i_l$ of MCL can be defined.

For TT2, in both ECL and MCL, we make use of $(S(z^i_{l+1}) + S(z^i_l))/2$ and $(S(z^{i+1}_l) + S(z^i_l))/2$ to substitute $S(z^i_{l+1/2})$ and $S(z^{i+1/2}_l)$, respectively. For the above each scheme, it is easy to verify that $(E^*_{le})^i_l = (E_{le})^i_l/(\tau h)$ and $(M^*_{le})^i_l = (M_{le})^i_l/(\tau h)$. According to Theorems 4.2 and 4.5, we have

$$|(E^*_{le})^i_l| \leqslant C\tau^2 \quad \text{and} \quad |(M^*_{le})^i_l| \leqslant Ch^2, \tag{5.4}$$

respectively, for applying MM2. Similarly, from Theorems 4.8 and 4.11, it follows that

$$|(E^*_{le})^i_l| \leqslant C(\tau^2 + h^2) \quad \text{and} \quad |(M^*_{le})^i_l| \leqslant C(\tau^2 + h^2), \tag{5.5}$$

respectively, for applying TT2.

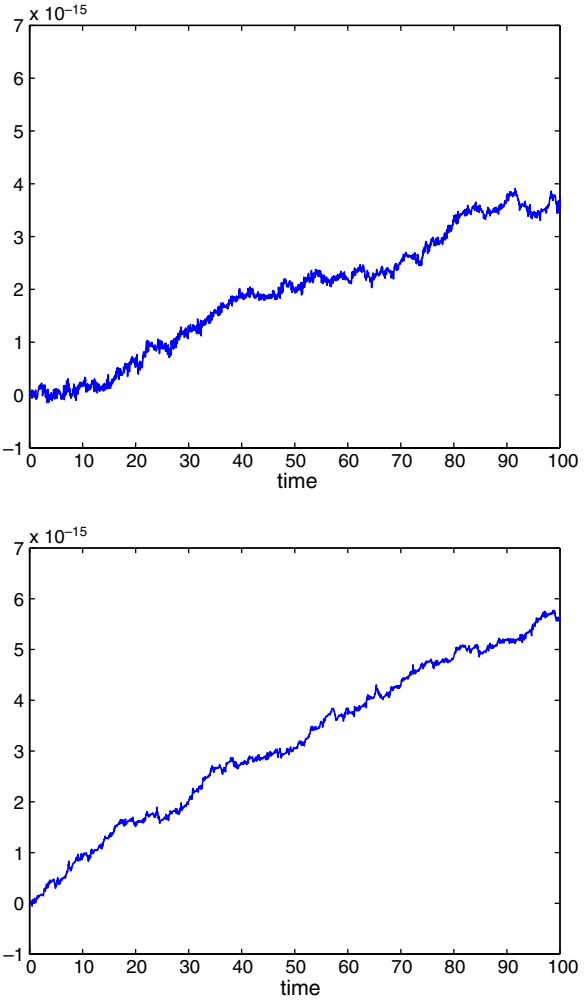

Fig. 5. The global errors of the discrete total momentum: MM2 (top); TT2 (bottom).

For each i, let $\max_{0\leqslant l<N}|(E^*_{le})^i_l|$ and $\max_{0\leqslant l<N}|(M^*_{le})^i_l|$ denote the maximum errors of the energy conservation law and the momentum conservation law, respectively. Fig. 2 exhibits the variation of $\max_{0\leqslant l<N}|(E^*_{le})^i_l|$ in the time interval [0,100], and shows that MM2 and TT2 have about the same numerical behaviors in the numerical preservation of the local energy conservation law, in fact, the energy error of MM2 is in the scale of 10^{-6}, one of TT2 in the scale of 10^{-5}. The stability of MM2 and TT2 with respect to the local energy conservation law is verified numerically.

Fig. 3 shows the variation of $\max_{0\leqslant l<N}|(M^*_{le})^i_l|$ in the time interval [0,100], and reveals that the difference between MM2 and TT2 in the error variation of the local momentum is not remarkable large, the error value with MM2 is about 1/2 of one with TT2. The oscillation curves in Fig. 3 shows numerically that MM2 and TT2 are stable in the sense of the local momentum conservation law. The numerical results in Figs. 2 and 3 are consistent with Theorems 4.2 and 4.3, respectively.

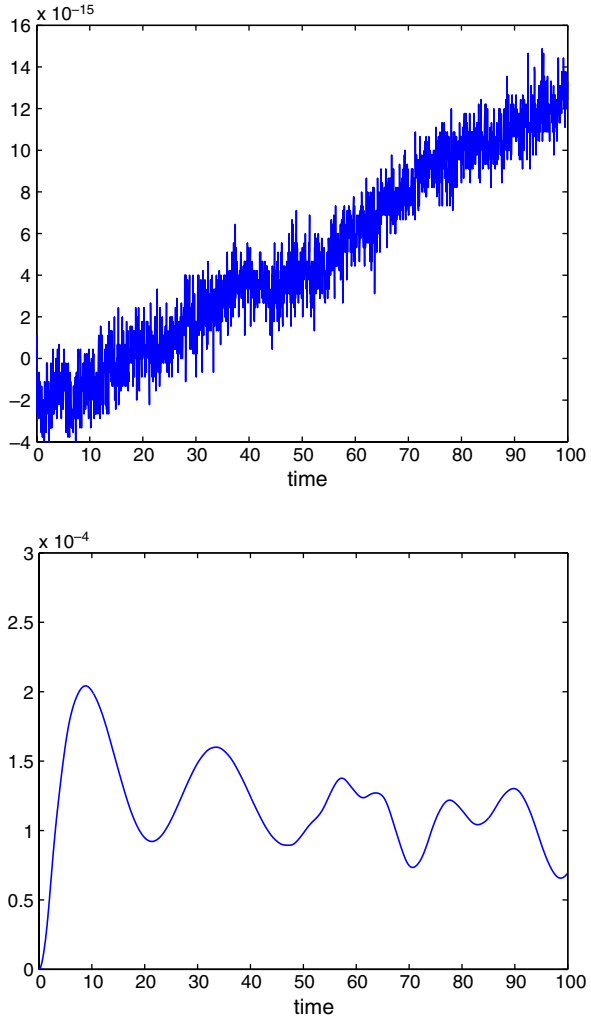

Fig. 6. The global errors of the discrete charge: MM2 (top); TT2 (bottom).

Fig. 4 exhibits the global error of the total energy (4.4), here $(\mathscr{E}_L^d)^i - (\mathscr{E}_L^d)^0$ denotes the global error of the total energy. $(\mathscr{I}_L^d)^i - (\mathscr{I}_L^d)^0$ denotes the global error of the total momentum (4.5), which is pictured in Fig. 5. Fig. 4 shows that the global error $(\mathscr{E}_L^d)^i - (\mathscr{E}_L^d)^0$ of the total energy obtained by using MM2 is not different from one obtained by using TT2, the numerical efficiency of the two methods is much the same, they produce the global error of total energy in the same magnitude. In the numerical simulation of total energy by using MM2, in the interval [0,25] the global error is in the scale of $\mathscr{O}(10^{-7})$. This means that the MM2 scheme preserves the total energy so well. It is out of our expectation that, in the interval [25,40], the global error has a sharp change, it reaches in the magnitude of $\mathscr{O}(10^{-5})$, and in the interval [40,100], the error changes more and more slowly. This numerical result motivates us to study theoretically the accumulation of $(\mathscr{E}_L^d)^i - (\mathscr{E}_L^d)^0$ in the application of MSRK methods to the Dirac equation.

Fig. 5 shows that the total momentum are conserved within roundoff errors of the computer not only by MM2, but also by TT2. $(\mathscr{I}_L^d)^i - (\mathscr{I}_L^d)^0$ is controlled in the scale of 10^{-15} by both of the two methods. The total momentum is a quadratic invariant which is different from that considered for ODEs, and it is in an integration form and the integrated function contains the terms of derivatives. The discrete invariance of the total momentum, under the discretizations of MM2 and TT2, is characterized numerically. The numerical results imply that both of two methods preserves the total momentum of the equation exactly. The corresponding theoretical discussion to this numerical phenomenon is proposed in [9].

Let $\mathscr{Q}^i - \mathscr{Q}^0$ denote the global error of the charge conservation law (CCL). Fig. 6 shows the global errors of CCL produced by both of the two schemes in the time interval [0,100]. The top graph in the figure shows that the discrete charge is conserved within roundoff errors of the computer by means of MM2, however, the global errors $\mathscr{Q}^i - \mathscr{Q}^0$ produced by using TT2 are in the scale of $\mathscr{O}(10^{-4})$. From the error estimates of the energy and momentum, we find that *the remarkable advantage of MSRK methods is the precise preservation of charge conservation law.* In Fig. 7, we exhibit the evolution of the global error of charge conservation law in a longer time interval [0,5000] by means of the numerical implementation of MM2. In the time interval, the discrete charge conservation law is preserved in the scale of $\mathscr{O}(10^{-13})$, almost the roundoff of the computer; comparing with the top graph in Fig. 6, there is a very small error accumulation in such long calculation. The numerical results of the discrete charge

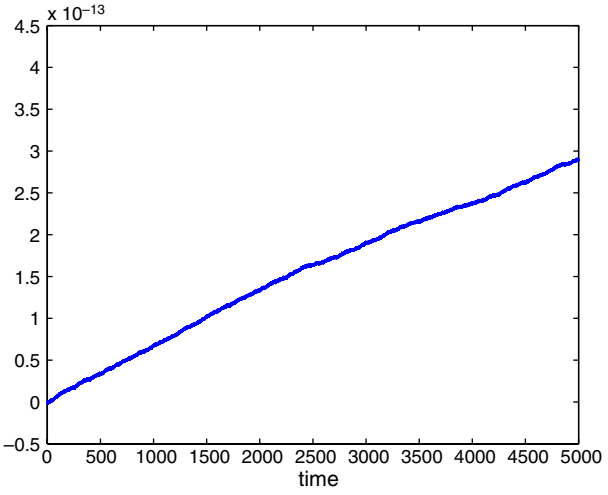

Fig. 7. The global error of the discrete charge in time interval [0,5000] obtained by using MM2.

conservation law in Figs. 6 and 7 reveal that, in the preservation of charge, MM2 is superior to TT2. The above numerical phenomena reveal that the superiority of MSRK methods is not only on the conservation of multi-symplectic geometric structure, but also on the preservation of some crucial conservative properties in quantum physics.

Now let us look at the rest of figures. Fig. 8 displays the maximum global errors of the wave function, here we make use of

$$\max_{0\leqslant l\leqslant N}\left(\max(|(p_1)_l^i - p_1(x_l,t_i)|, |(q_1)_l^i - q_1(x_l,t_i)|, |(p_2)_l^i - p_2(x_l,t_i)|, |(q_2)_l^i - q_2(x_l,t_i)|)\right)$$

to denote the maximum global error of the wave function, where $(p_1)_l^i$ is the numerical solution of the first component $p_1(x,t)$ at (x_l,t_i), and $p_1(x_l,t_i)$ is the value of the function p_1 at (x_l,t_i). The two graphs in Fig. 8 shows that the maximum global errors obtained by using MM2 and TT2, respectively, are in reasonable oscillation and in normal linear growth.

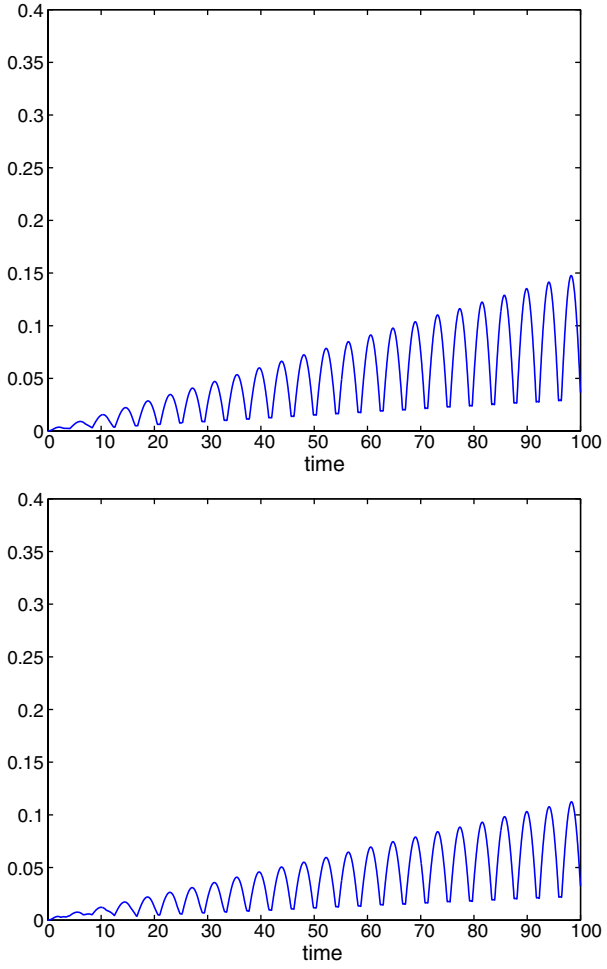

Fig. 8. The maximum global errors of the wave function: MM2 (top); TT2 (bottom).

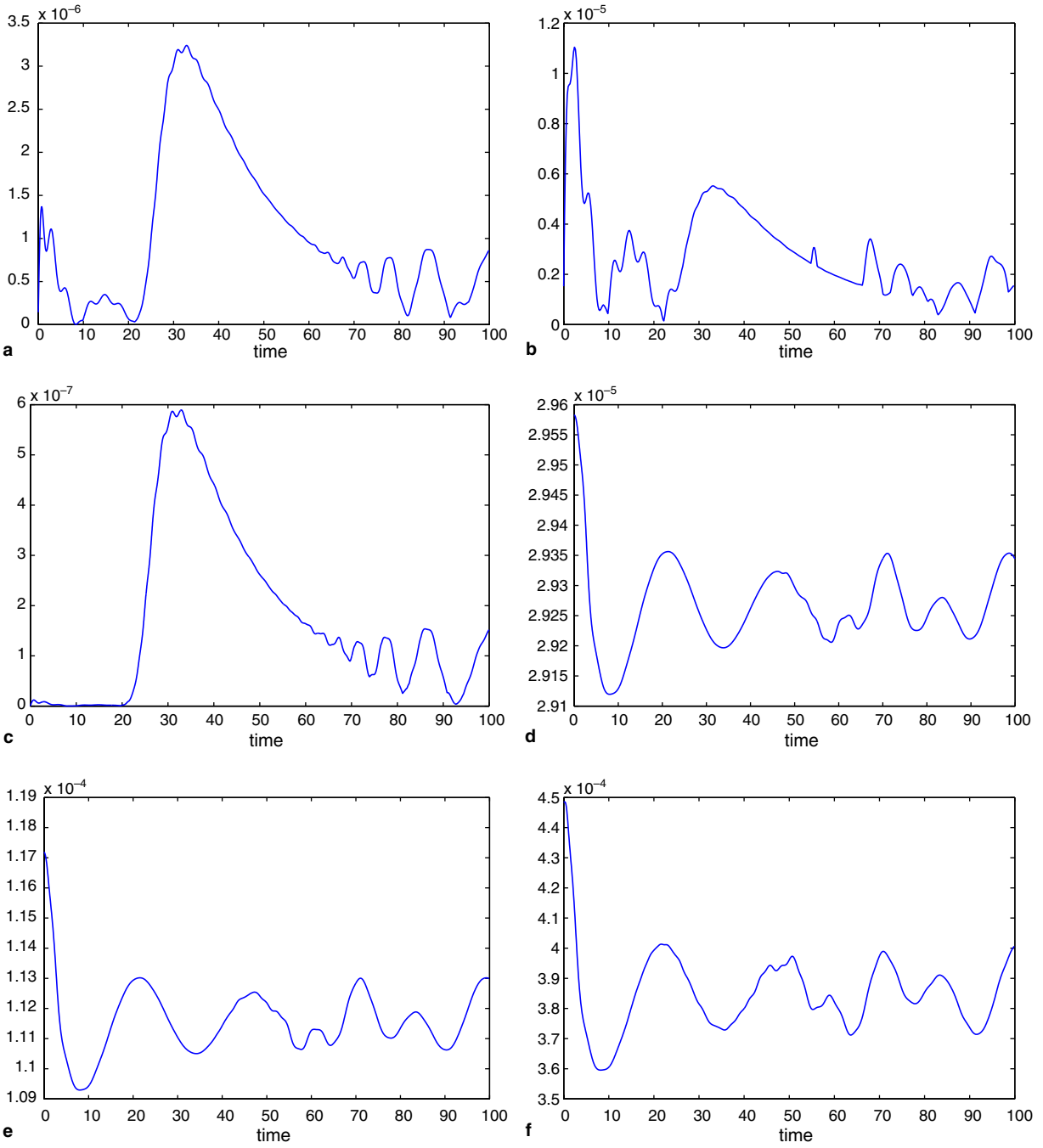

Fig. 9. The maximum errors of ECL and MCL obtained by using MM2 with different spatial and temporal stepsizes: (a) ECL, $h = 0.3$ and $\tau = 0.1$; (b) ECL, $h = 0.3$ and $\tau = 0.2$; (c) ECL, $h = 0.3$ and $\tau = 0.025$; (d) MCL, $h = 0.15$ and $\tau = 0.05$; (e) MCL, $h = 0.3$ and $\tau = 0.1$; (f) MCL, $h = 0.6$ and $\tau = 0.1$.

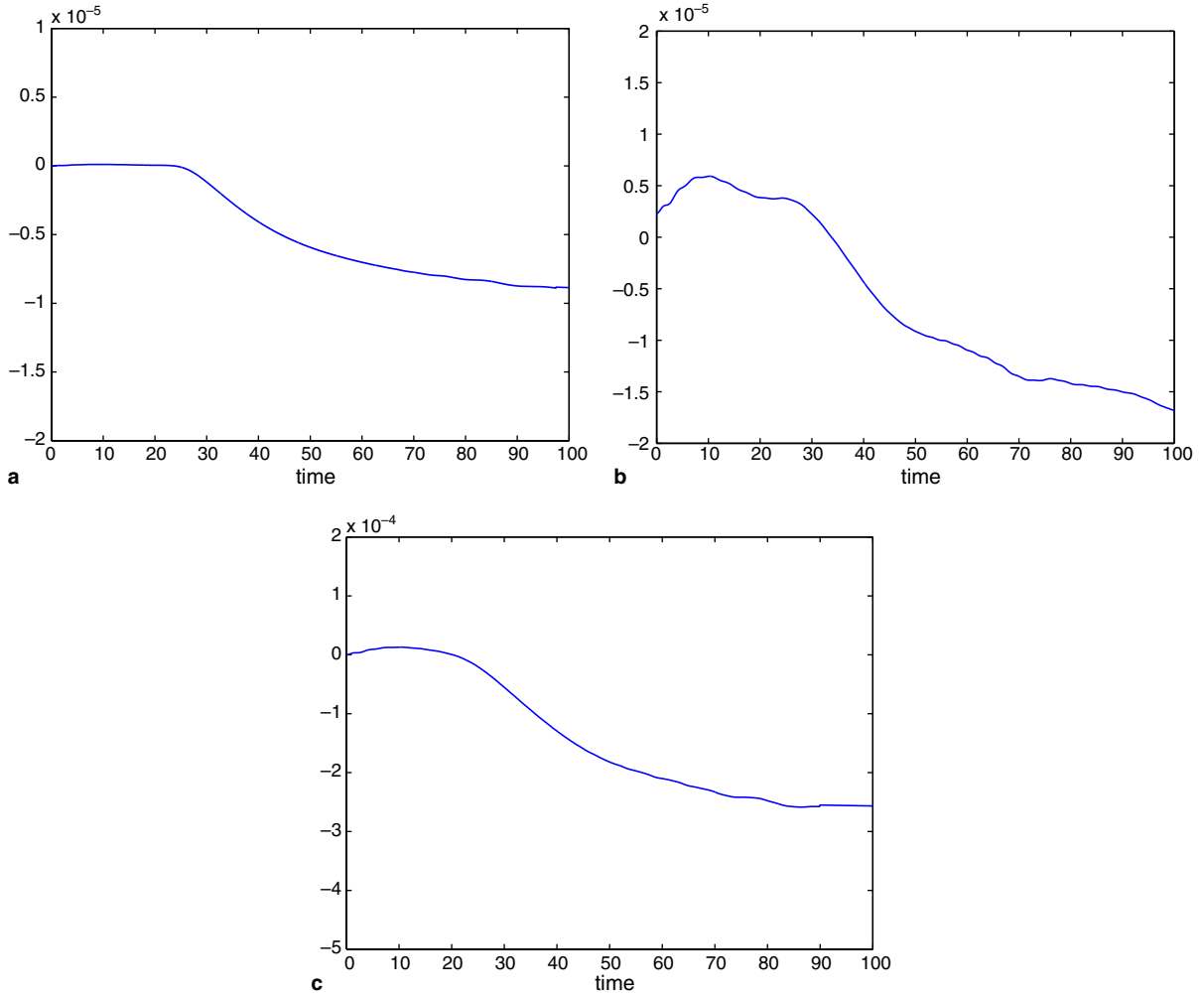

Fig. 10. The global errors of the discrete total energy obtained by using MM2 with different spatial and temporal stepsizes: (a) $h = 0.3$ and $\tau = 0.025$; (b) $h = 0.3$ and $\tau = 0.1$; (c) $h = 0.3$ and $\tau = 0.2$.

Figs. 1–8 are obtained by taking $h = 0.3$ and $\tau = 0.05$. In Figs. 9–12, we take different stepsizes to numerically verify theoretical results on the error estimates, presented in Section 4.

Fig. 9 shows the maximum errors of ECL ((a), (b) and (c)) and MCL ((d), (e) and (f)) obtained by taking different stepsizes. It is observed that numerical results are consistent with theoretical ones in Section 4.2.

Fig. 10 shows the global errors of the discrete total energy by making use of MM2 with fixed spatial stepsize $h = 0.3$ and different temporal sizes. The numerical result coincides with the corresponding one on the error estimate in Section 4.2. Fig. 11 shows the evolution of the maximum errors of ECL and MCL by TT2 with different stepsizes. Fig. 12 exhibits the global errors of the charge and the total energy obtained by TT2. Numerical experiments show the match between numerical results and theoretical ones in Section 4.

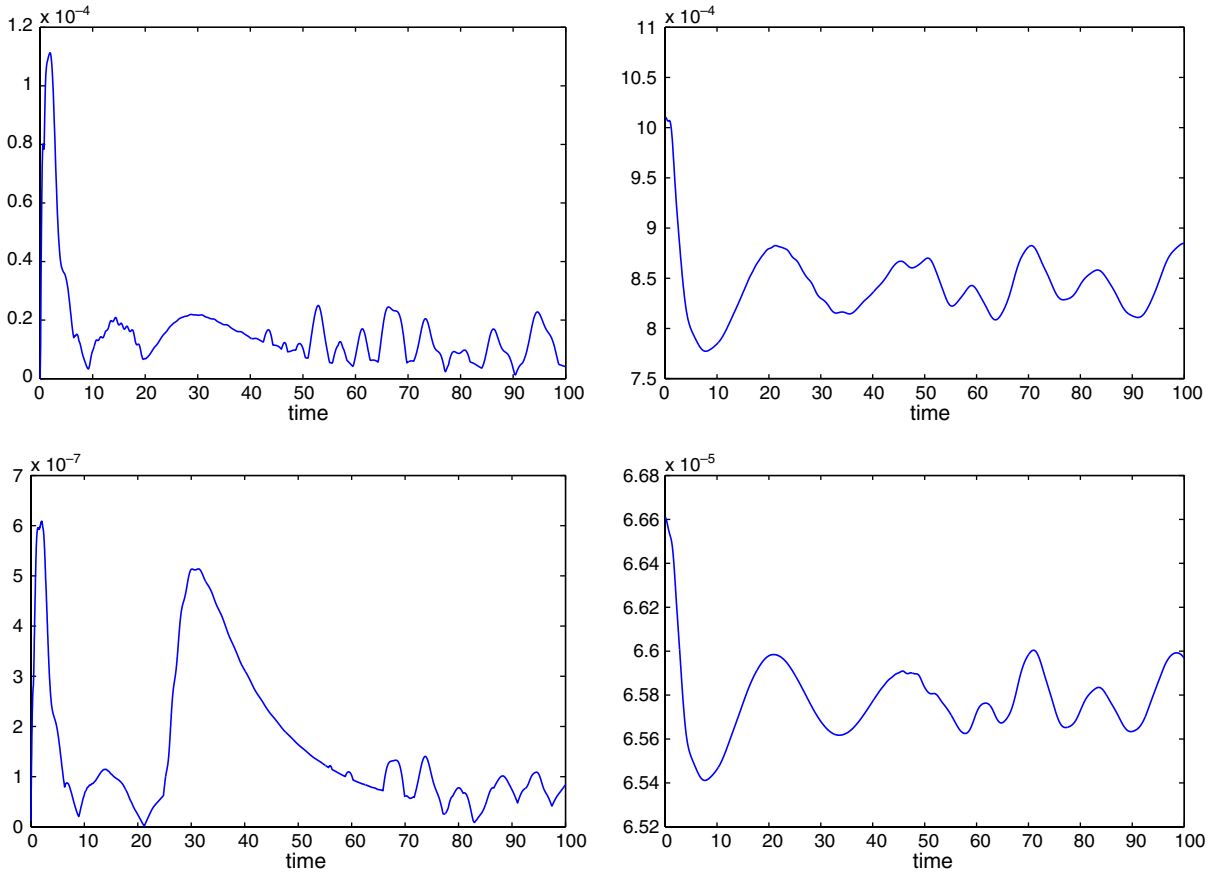

Fig. 11. The maximum errors of ECL and MCL obtained by using TT2: $h = 0.6$ and $\tau = 0.1$ (top); $h = 0.15$ and $\tau = 0.025$ (bottom); ECL (left); MCL (right).

6. Conclusions

For the Runge–Kutta discretization of the nonlinear Dirac equation, the symplecticity both in time and space directions implies the multi-symplecticity of the integrator. This result is true for the general multi-symplectic Hamiltonian PDEs in the form (2.2). Investigating the preservation of charge, energy and momentum of the nonlinear Dirac equation under the structure-preserving discretization is very important. Our conclusions are listed as follows:

- Theorems 4.2 and 4.3 imply that for a MSRK method applied to the nonlinear Dirac equations under appropriate conditions, there exists a constant $C > 0$ such that for sufficient small τ and h, we have

$$|E_{le} + M_{le}| \leqslant C\tau h(\tau^2 + h^2), \tag{6.1}$$

which reflects the local symmetry of energy and momentum under the discretization of MSRK method (3.3). The superposition of error curves in Figs. 2 and 3 verifies numerically the local symmetry (6.1).

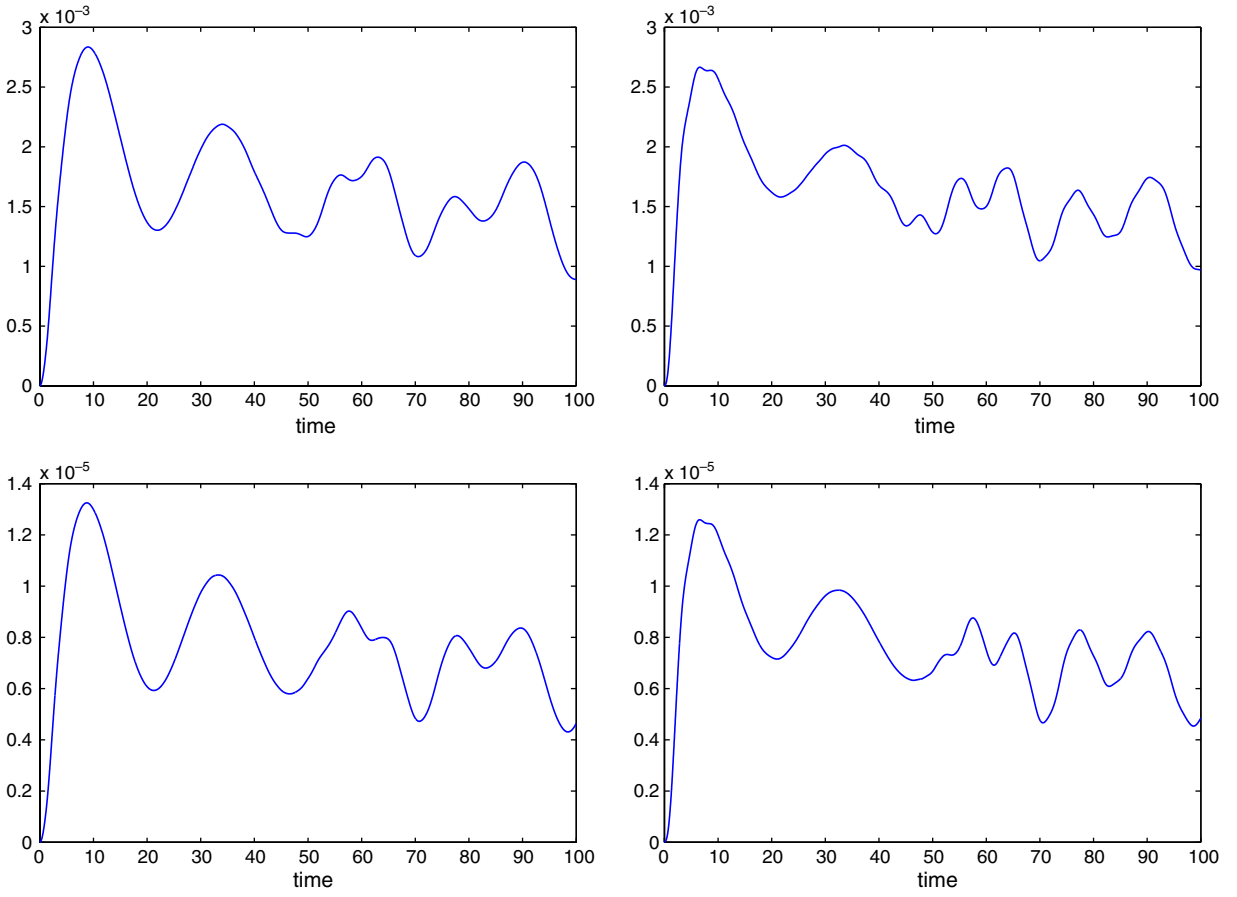

Fig. 12. The global errors of the discrete charge and the total energy obtained by using TT2: $h = 0.6$ and $\tau = 0.1$ (top); $h = 0.15$ and $\tau = 0.025$ (bottom); the discrete charge (left); the discrete total energy (right).

- Numerical experiments exhibit that the MSRK methods applied to the nonlinear Dirac equations are stable in the sense of energy, momentum and charge, in particular, they preserve exactly the conservation laws of momentum and charge in the sense of corresponding discretization. Numerical results motivate us to study theoretically the accumulation of $(\mathscr{E}_L^d)^i - (\mathscr{E}_L^d)^0$ in the application of MSRK methods to the numerical computation of relativistic quantum physics.
- In the numerical comparisons, it is shown that MM2 has the same efficiency as TT2 on the numerical simulation of solitary waves and the preservation of the conservation laws of energy and momentum, and it is superior to TT2 on the preservation of the charge conservation law which is a crucial conservative property in quantum physics. This implies that *MSRK methods preserve not only the inner symmetry, the multi-symplectic geometric structure, but also some crucial conservative properties in the relativistic quantum physics.*

Numerical results in Section 5 comport with theoretical ones in Section 4, and infer that MSRK methods applied to the nonlinear Dirac equations should preserve exactly the conservation law of global momentum. Numerical experiments elicit a further theoretical investigation in numerical mathematics, thus our work is just at the beginning.

Acknowledgment

The authors are grateful to the referee for his valuable comments.

References

[1] A. Alvarez, Linear Crank–Nicholsen scheme for nonlinear Dirac equations, J. Comput. Phys. 99 (1992) 348–350.
[2] A. Alvarez, B. Carreras, Interaction dynamics for the solitary waves of a nonlinear Dirac model, Phys. Lett. 86A (1981) 327–332.
[3] A. Alvarez, P. Kuo, L. Vazquez, The numerical study of a nonliear one-dimensional Dirac equation, Appl. Math. Comput. 13 (1983) 1–15.
[4] T.J. Bridges, S. Reich, Multi-symplectic integrators: numerical schemes for Hamiltonian PDEs that conserve symplecticity, Phys. Lett. A 284 (2001) 184–193.
[5] J. de Frutos, J.M. Sanz-Serna, Split-step spectral schemes for nonlinear Dirac systems, J. Comput. Phys. 83 (1989) 407–423.
[6] J. Hong, H. Liu, G. Sun, The multi-symplecticity of partitioned Runge–Kutta methods for Hamiltonian PDEs, Math. Comput. (2005), in press.
[7] J. Hong, Y. Liu, Multi-symplecticity of the central box scheme for a class of Hamiltonian PEDs and a application to quasi-periodically solitary waves, Math. Comput. Model 39 (2004) 1035–1047.
[8] J. Hong, Y. Liu, A novel numerical approach to simulating nonlinear Schrödinger equations with varying coefficients, Appl. Math. Lett. 16 (2003) 759–765.
[9] J. Hong, C. Li, Some properties of multi-symplectic Runge–Kutta methods for Dirac equations, Research Report of ICMSEC, 2004.
[10] A. Iserles, A First Course in the Numerical Analysis of Differential Equations, Cambridge University Press, Cambridge, 1996.
[11] A.L. Islas, D.A. Karpeev, C.M. Schober, Geometric integrators for the nonlinear Schrödinger equation, J. Comput. Phys. 173 (2001) 116–148.
[12] A.L. Islas, C.M. Schober, On the preservation of phase space structure under multisymplectic discretization, J. Comput. Phys. 197 (2004) 585–609.
[13] J.E. Marsden, G.W. Patrick, S. Shkoller, Multisymplectic geometry variational integrators, and nonlinear PDEs, Comm. Math. Phys. 199 (1998) 351–395.
[14] J.E. Marsden, S. Pekarsky, S. Shkoller, M. West, Variational methods, multisymplectic geometry and continuum mechanics, J. Geo. Phys. 38 (3-4) (2001) 253–284.
[15] J.E. Marsden, T.S. Ratiu, Introduction to Mechanics and Symmetry, second ed., Springer, Germany, 1999.
[16] B. Moore, S. Reich, Multisymplectic integration methods for Hamiltonian PDEs, Future Gener. Comput. Syst. 19 (2003) 395–402.
[17] B. Moore, S. Reich, Backward error analysis for multi-symplectic integration methods, Numer. Math. 95 (2003) 625–652.
[18] M. Oliver, M. West, C. Wulff, Approximate momentum conservation for spatial semidiscretizations of semilinear wave equations, 2004, preprint. Available from: <http://www.maths.surrey.ac.uk/personal/st/C.Wulff/>.
[19] S. Reich, Multi-symplectic Runge–Kutta collocation methods for Hamiltonian wave equation, J. Comput. Phys. 157 (2000) 473–499.
[20] J.M. Sanz-Serna, M.P. Calvo, Numerical Hamiltonian Problems, Chapman & Hall, London, 1994.